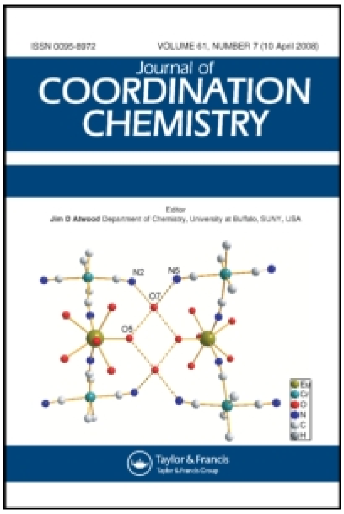

Journal of Coordination Chemistry
Publication details, including instructions for authors and subscription information:
http://www.informaworld.com/smpp/title~content=t713455674

Spectral, magnetic, biological, and thermal studies of metal(II) complexes of some unsymmetrical Schiff bases

A. A. Nejo[a]; G. A. Kolawole[a]; M. C. Dumbele[a]; A. R. Opoku[b]
[a] Department of Chemistry, University of Zululand, South Africa [b] Department of Biochemistry and Microbiology, University of Zululand, South Africa

First published on: 07 December 2010

To cite this Article Nejo, A. A. , Kolawole, G. A. , Dumbele, M. C. and Opoku, A. R.(2010) 'Spectral, magnetic, biological, and thermal studies of metal(II) complexes of some unsymmetrical Schiff bases', Journal of Coordination Chemistry, 63: 24, 4367 — 4379, First published on: 07 December 2010 (iFirst)

To link to this Article: DOI: 10.1080/00958972.2010.539684
URL: http://dx.doi.org/10.1080/00958972.2010.539684

Journal of Coordination Chemistry
Vol. 63, No. 24, 20 December 2010, 4367–4379

Spectral, magnetic, biological, and thermal studies of metal(II) complexes of some unsymmetrical Schiff bases

A.A. NEJO†, G.A. KOLAWOLE*†, M.C. DUMBELE† and A.R. OPOKU‡

†Department of Chemistry, University of Zululand, South Africa
‡Department of Biochemistry and Microbiology, University of Zululand, South Africa

(*Received 5 August 2010; in final form 22 October 2010*)

New nickel(II) and copper(II) complexes with unsymmetrical Schiff bases derived from aromatic 2-hydroxy aldehydes were synthesized and characterized by elemental analyses, melting points, ^{1}H-NMR, magnetic susceptibility, thermogravimetric analysis, differential scanning calorimetry (DSC), infrared (IR), and electronic spectral measurements. Comparison of IR spectra of the Schiff bases and their metal complexes indicated that the Schiff bases are tetradentate, coordinated *via* the two azomethine nitrogens and the two phenolic oxygens. Magnetic moments and electronic spectral data confirm square-planar geometry for the complexes. Thermal studies reveal a general decomposition pattern, whereby the complexes decomposed partially in a single step due to loss of part of the organic moiety. A single endothermic profile, corresponding to melting point, was observed from the DSC of all complexes, except those whose ligand contained the nitro group, which decomposed exothermally without melting. The Schiff bases and their complexes were screened *in vitro* against 10 human pathogenic bacteria. The metal(II) complexes exhibited higher antibacterial activity than their corresponding Schiff bases.

Keywords: Nickel(II); Copper(II); Unsymmetrical Schiff base; Antibacterial studies

1. Introduction

Nitrogen and sulfur donors play key roles in the coordination of metals at the active sites of numerous metallobiomolecules [1]. Schiff-base metal complexes have been widely studied because they have industrial, antifungal, antibacterial, anticancer, antiviral, and herbicidal applications [2–7], serve as models for biologically important species, and find applications in biomimetic catalytic reactions. Chelating ligands containing N, S, and O donors show broad biological activity and are of special interest because of the variety of ways in which they are bonded to metal ions. Coordination of metal ions to biologically active compounds may enhance their activities [5–7].

The structure and mechanism of the formation of Schiff-base complexes and the stereochemistry of four-coordinate chelate complexes formed from Schiff bases and their analogues have been discussed in reviews [8–11]. The configuration of the four-coordinate complexes may be square planar, tetrahedral, distorted tetrahedral, or

---

*Corresponding author. Email: gayokola@pan.uzulu.ac.za

Journal of Coordination Chemistry
ISSN 0095-8972 print/ISSN 1029-0389 online
DOI: 10.1080/00958972.2010.539684

distorted trigonal pyramidal depending primarily on the nature of the metal and the magnitude and symmetry of the ligand field. Metal complexes have also been reported with other ligands mixed with Schiff bases. Of all the Schiff base complexes, symmetrically coordinated salicylaldiimines have attracted greater attention. A variety of physiochemical investigations on these complexes provide a clear understanding of their stereochemical and electronic properties. The advantage of the salicylaldiimine ligand system is the considerable flexibility of the synthetic procedures, which have resulted in the preparations of a wide variety of complexes with a given metal whose properties are often dependent on the ligand structure.

We have recently reported oxovanadium(IV) complexes with the same series of unsymmetrical Schiff bases as in this article [12]. The enhancement of glucose uptake of the oxovanadium(IV) complexes revealed some structure–activity relationships of the substituents on the salicylaldehyde group, whereby plasma glucose uptake was related to the electronic properties of the substituents. We report here the physical, structural, antibacterial, and thermal properties of nickel(II) and copper(II) complexes of four unsymmetrical Schiff bases. The complexes investigated are reported for the first time.

2. Experimental

2.1. *Materials*

Ethanol, methanol, chloroform, dimethylsulfoxide, salicylaldehyde, 5-chlorosalicylaldehyde, 5-nitrosalicylaldehyde, 3-ethoxysalicylaldehyde, 2-hydroxy-1-naphthaldehyde, copper(II) acetate monohydrate, nickel(II) acetate tetrahydrate, and *o*-phenylenediamine are of Analar grade and were used as purchased from Aldrich–Sigma company.

2.2. *Preparation of the compounds*

The procedure for the preparation of the unsymmetrical Schiff bases was reported elsewhere [12]. The metal(II) complexes were prepared by the addition of 3 mmol of $Ni(CH_3COO)_2{\cdot}4H_2O$ (0.53 g) or $Cu(CH_3COO)_2{\cdot}H_2O$ (0.59 g), dissolved in hot absolute methanol (60 mL), to a stirring 3 mmol of the respective Schiff base in methanol (40 mL). The color of the mixture changed instantly. The mixture was refluxed for 3 h and the colored precipitates were filtered, washed with cold methanol, and allowed to dry in a desiccator over silica gel.

2.3. *Physical measurements*

Elemental analyses were performed using a Perkin-Elmer model 2400 Series II CHNS/O elemental analyzer. Infrared (IR) spectra of the ligands and complexes were recorded on a Bruker FT-IR (ATR) tensor 27 spectrophotometer directly on small samples of the compounds from 200 to 4000 cm^{-1}. ^1H NMR spectra of the ligands were previously reported [12]. Electronic absorption spectra of the complexes were recorded from 200 to 1100 nm on freshly prepared $CHCl_3$ and DMSO solutions using a Cary Model 50 spectrophotometer. Melting points were determined on a Barnstead/electrothermal digital melting point apparatus and are uncorrected. Magnetic susceptibility measurements were made on powdered samples using a Sherwood Scientific magnetic susceptibility balance. $Hg[Co(SCN)_4]$ was used as the calibrant and corrections for diamagnetism were calculated from Pascal's constants. Thermogravimetric analysis (TGA) was carried out at 15°C min^{-1} heating rate using a Perkin-Elmer Pyris 6 TGA under nitrogen up to 700°C with a closed perforated aluminum pan. The differential scanning calorimetry (DSC) analysis was carried out at 20°C min^{-1} heating rate up to 450°C under nitrogen using a Perkin-Elmer DSC 4000 series, which was calibrated with indium metal.

2.4. *Biological studies*

Ten pathogenic bacteria (Gram negative and Gram positive), namely *Escherichia coli* (ATCC 8739), *Pseudomonas aeruginosa* (ATCC 19582), *Acinetobacter calcoaceuticus anitratus* (Aci2), *Shigella flexneri*, *Salmonella* spp., *Staphylococcus aureus* (ATCC 6538), *Streptococcus faecalis* (ATCC 29212), *Bacillus subtilis*, *Staphylococcus epidermidis*, and *Micrococcus kristinae* were collected from the Department of Microbiology, University of Fort Hare, South Africa. Antibacterial activities of the ligands and metal complexes were carried out using the disc diffusion method described by Bauer *et al.* [13]. Bacteria were maintained on Mueller–Hinton nutrient agar at 4°C. Molten Mueller–Hinton agar was inoculated with a broth culture of the respective bacterial strains and poured over sterile 90 mm Petri dishes. Both metal complexes and ligands were dissolved in DMSO to a final concentration of 10 mg mL^{-1}. Sterile Whatman No. 1 (6 mm) disc were separately impregnated with each sample to be tested at 5.0 mg mL^{-1} and placed on the inoculated agar. The plates were incubated at 37°C for 24 h and zones of inhibition were measured at the end of the incubation period. The standard antibiotic reference drug used is chloramphenicol.

3. Results and discussion

3.1. *Synthesis*

A series of new unsymmetrical tetradentate Schiff-base complexes of nickel(II) and copper(II) were prepared by refluxing the relevant unsymmetrical Schiff bases with the corresponding metal(II) acetate in methanol at 1 : 1 mole ratio as in the scheme presented in figure 1. All the metal complexes are stable, non-hygroscopic, insoluble in common organic solvents but partly soluble in chloroform and DMSO. The unsymmetrical Schiff-base complexes did not melt or decompose when heated to 250°C. The purity of the Schiff bases and their metal complexes as formulated were established by microanalyses. Although crystal structures are not available, the proposed structures are consistent with all other evidence. The analytical data, color, percentage yields, melting points, and magnetic moments of the compounds are presented in table 1.

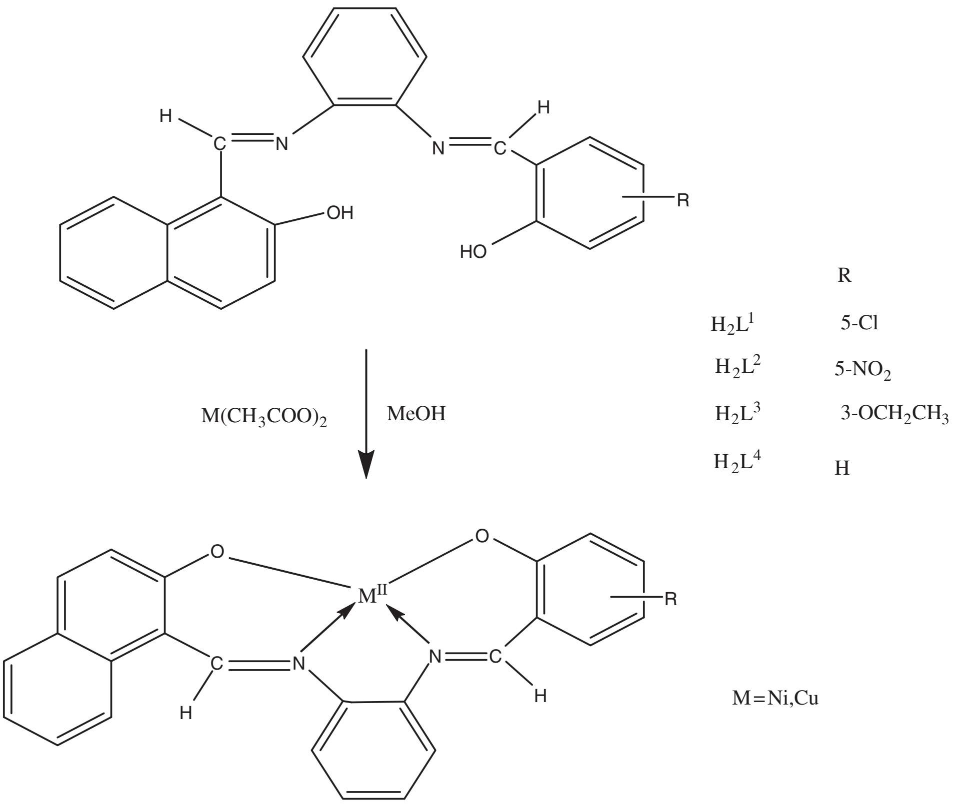

Figure 1. Preparation of the metal complexes from the Schiff bases.

3.2. *IR spectra*

The positions of the important bands of the compounds are shown in table 2. Tentative assignments of the observed bands for the compounds were made by comparing spectra of the metal complexes with those of the Schiff bases. Due to the unsymmetrical nature of ligands and the complexes two bands were observed for each of the following bonds, ν(C=N), ν(C–O), ν(M–N), and ν(M–O) taking their origin from the different aldehydes [12]. The ligands exhibited characteristic C=N stretching frequency at 1610–1621 and 1567–1583 cm^{-1}, which shift to lower frequencies at 1603–1609 and 1577–1582 cm^{-1}, respectively, upon complexation. This indicates participation of the azomethine nitrogen in bonding [14]. The corresponding phenolic C–O stretching frequency occurs at 1313–1333 and 1276–1289 cm^{-1} for the ligands and at 1325–1366 and 1287–1317 cm^{-1} for the complexes. The shift confirms participation of the phenolic O in C–O–M bond formation [15]. Thus, it can be concluded that the Schiff bases are tetradentate, coordinating *via* the azomethine *N* and the phenolic *O*.

It has also been reported that the metal–ligand vibrational modes are very sensitive to substituent effects from isotopic labeling studies [16, 17]. The substituent effects were based on the position of substitution rather than the nature of the substituents.

Table 1. Physical properties, analytical data, and magnetic moments of the compounds.

Compound	Molecular formula (formula mass)	Yield (%)	Color	m.p. (°C)	Microanalysis (Calcd)			μ_{eff} (BM)
					%C	%H	%N	
H_2L^1	$C_{24}H_{17}N_2O_2Cl$ (400.58)	91.5	Orange-yellow	194–195	71.60 (71.90)	4.73 (4.28)	6.60 (6.99)	
NiL^1	$C_{24}H_{15}N_2O_2ClNi$ (457.26)	95.8	Red	>250	63.21 (62.98)	3.22 (3.31)	5.87 (6.12)	0
CuL^1	$C_{24}H_{15}N_2O_2ClCu$ (462.11)	90.9	Pale Brown	>250	62.06 (62.32)	3.11 (3.27)	5.68 (6.06)	2.20
H_2L^2	$C_{24}H_{17}N_3O_4$ (411.12)	86.2	Orange-yellow	134–135	69.69 (70.05)	4.23 (4.17)	10.12 (10.22)	
NiL^2	$C_{24}H_{15}N_3O_4Ni$ (467.80)	96.1	Red	>250	61.02 (61.56)	3.16 (3.23)	8.87 (8.98)	0
CuL^2	$C_{24}H_{15}N_3O_4Cu$ (472.65)	86.3	Pale Brown	>250	60.72 (60.93)	3.47 (3.20)	9.13 (8.89)	1.56
H_2L^3	$C_{26}H_{22}N_2O_3$ (410.16)	71.9	Orange-yellow	135–136	76.34 (76.07)	5.51 (5.41)	6.79 (6.83)	
NiL^3	$C_{26}H_{20}N_2O_3Ni$ (466.84)	90.2	Red	>250	66.49 (66.83)	4.17 (4.32)	5.51 (6.00)	0
CuL^3	$C_{26}H_{20}N_2O_3Cu$ (471.69)	91.7	Pale Brown	>250	66.03 (66.14)	4.50 (4.27)	5.48 (5.94)	1.81
H_2L^4	$C_{24}H_{18}N_2O_2$ (366.14)	78.4	Orange-yellow	187–188	78.41 (78.66)	4.81 (4.95)	7.62 (7.65)	
NiL^4	$C_{24}H_{16}N_2O_2Ni$ (422.81)	88.8	Red	>250	68.11 (68.12)	3.70 (3.81)	6.31 (6.62)	0
CuL^4	$C_{24}H_{16}N_2O_2Cu$ (427.68)	94.8	Pale Brown	>250	66.98 (67.34)	3.86 (3.77)	6.38 (6.55)	1.78

Table 2. Selected IR spectral bands of the compounds.

Complex	ν(C=N)	ν(C–O)	ν(M–N)	ν(M–O)
NiL^1	1609, 1582	1331, 1287	457, 431	577, 554
CuL^1	1606, 1582	1325, 1290	457, 419	574, 548
H_2L^1	1611, 1583	1313, 1276	–	–
NiL^2	1603, 1580	1366, 1311	457, 431	545, 510
CuL^2	1606, 1580	1363, 1317	472, 452	563, 501
H_2L^2	1621, 1567	1333, 1289	–	–
NiL^3	1606, 1577	1346, 1290	478, 431	560, 507
CuL^3	1606, 1580	1340, 1311	498, 463	560, 542
H_2L^3	1610, 1569	1316, 1283	–	–
NiL^4	1606, 1577	1343, 1290	583, 507	463, 431
CuL^4	1606, 1580	1340, 1311	574, 545	460, 416
H_2L^4	1615, 1568	1313, 1286	–	–

The ν(M–O) bands are observed to exhibit higher vibrational frequencies than the ν(M–N) bands for the *meta*-substituents, while the order is reversed for *para*-substituents regardless of the nature of the substituents. The substituents in the complexes reported in this study are located in the 3- and 5-positions on the salicylaldehyde ring and it is expected that ν(M–O) bands would be greater than ν(M–N) bands, as shown in table 2. Assignments of ν(M–O) bands in the *meta*-substituted complexes are located at 501–557 and 545–577 cm^{-1}, while ν(M–N) bands are at 419–463 and 457–498 cm^{-1}. Corresponding assignments for ML^4 are at 416–431 and 460–463 cm^{-1} (for ν(M–O)) and 507–545 and 574–583 cm^{-1} (for ν(M–N)).

3.3. *Electronic spectra*

Electronic absorption spectra of the metal(II) complexes were recorded in 10^{-5} mol L^{-1} solutions of each complex in DMSO and chloroform from 200 to 1100 nm at room temperature and their results are presented in table 3.

Solution spectra of all the nickel(II) complexes in both solvents are very similar consisting of four bands. The electronic spectra in $CHCl_3$ show two bands at 20,619–20,747 and 25,773–26,178 cm^{-1} assignable to $^1A_{1g} \rightarrow {}^1B_{1g}$ and $^1A_{1g} \rightarrow {}^1E_g$ transitions in a square-planar geometry [18, 19]. The assignment of square-planar geometry is supported by the diamagnetism of the complexes. The stereochemistry of these complexes was unchanged when moving from a non-coordinating solvent to a coordinating solvent (DMSO) except for [NiL^2], whose ligand contains the nitro group, which suffered some minor distortion and gained intensity in DMSO. The observed bands in this complex were still in conformity with square-planar geometry. Solution spectra of the complexes in DMSO also show two bands at 20,619–20,877 and 25,974–26,178 cm^{-1}. At higher energy, two more intense absorptions are observed in the range 30,303–38,760 ($CHCl_3$) and 30,395–39,063 cm^{-1} (DMSO), which are likely due to charge transfer or intra-ligand transitions.

Electronic spectra of the copper(II) complexes in both $CHCl_3$ and DMSO show a broad unsymmetrical band centered at 22,831–24,038 and 23,095–24,038 cm^{-1}, respectively. This broad band is assigned to the $^2B_{1g} \rightarrow {}^2A_{1g}$ transition of four-coordinate, square-planar geometry [19, 20]. This d–d transition is in the region

Table 3. Electronic spectral data of the metal(II) complexes.

Compound	Solvent	d–d transitions/cm^{-1} (ϵ/cm^{-1} mol^{-1})	C.T.	Ligand[a]
NiL^1	CHCl$_3$	20,619 (154), 25,840 (361)	30,675 (211)	38,314 (697)
	DMSO	20,790 (145), 26,042 (322)	30,581 (183)	39,063 (658)
NiL^2	CHCl$_3$	20,704 (127), 26,178 (312)	30,769 (204)	38,760 (437)
	DMSO	20,877 (156), 26,178 (384)		31,250 (216) 38,610 (501)
NiL^3	CHCl$_3$	20,619 (162), 25,773 (383)	30,303 (234)	38,314 (700)
	DMSO	20,619 (161), 25,974 (375)	30,395 (232)	38,168 (830)
NiL^4	CHCl$_3$	20,747 (173), 25,840 (402)	30,675 (234)	38,314 (703)
	DMSO	20,877 (150), 26,110 (340)	30,581 (191)	38,168 (638)
CuL^1	CHCl$_3$	23,041 (280)	27,778 (176) 29,326 (198)	31,056 (240) 37,736 (482)
	DMSO	23,256 (307)	30,030 (215)	31,646 (223) 37,313 (529)
CuL^2	CHCl$_3$	24,038 (184)	28,571 (213)	31,447 (225) 36,900 (344) 40,816 (371)
	DMSO	23,981 (362)		36,101 (356)
CuL^3	CHCl$_3$	22,831 (262)	29,674 (269)	37,736 (421)
	DMSO	23,095 (262)	30,030 (252)	36,765 (408)
CuL^4	CHCl$_3$	23,416 (308)	27,933 (203)	31,250 (262) 38,168 (438)
	DMSO	23,585 (322)	28,490 (181) 30,395 (244)	

[a] The spectra were noisy in the UV and some of the bands in the region could not be extracted.

of that observed for structurally well-characterized complexes of copper(II) *N*-alkylsalicyladiminates with square-planar geometry [20]. The other intense bands between 27,778 and 40,816 cm^{-1} in CHCl$_3$ and 28,490−37,313 cm^{-1} in DMSO are due to charge transfer or intra-ligand transitions.

3.4. *Magnetic susceptibilities*

Nickel(II) has 3d^8 electronic configuration and should exhibit a magnetic moment higher than expected for two unpaired electrons in octahedral (2.8–3.2 B.M.) and tetrahedral (3.4–4.2 B.M.) complexes. Deviations from spin-only moment of 2.83 B.M. due to two unpaired electrons are attributed to orbital contributions. However, nickel(II) square-planar complexes are generally diamagnetic [19]. The observed diamagnetism confirms the square-planar environment for the nickel(II) complexes (table 1).

The room temperature magnetic moments of copper(II) complexes are expected to be higher than the spin-only value of 1.73 B.M. as a result of orbital contribution and spin–orbit coupling, which mixes in the higher T terms into the ground term. Consequently, the magnetic moments of 1.7–2.2 B.M. are usually observed for mononuclear copper(II) complexes, regardless of stereochemistry. The magnetic moments of 1.56–2.20 B.M. observed for the copper(II) complexes are assigned to four-coordinate, square-planar geometry [20].

Table 4. Thermoanalytical results (TGA, DSC) of the metal(II) complexes.

Compound	T^a (°C)	Weight loss^a (Calcd) (%)	Endothermic $t_{min}{}^b$ (°C)	Endothermic ΔH^b (Jg^{-1})	Exothermic $t_{max}{}^b$ (°C)	Exothermic ΔH^b (Jg^{-1})	Decomposition assignment
CuL^1	376.9	23.8 (22.3)	381.5	15.4	386.5	−203.8	C_6H_4, HCN
CuL^2	380.4	22.4 (21.8)	–	–	380.2	−228.4	C_6H_4, HCN
CuL^3	318.0	41.5 (42.6)	265.3	32.1	349.4	−39.9	C_6H_4, 2HCN, C_2H_2
CuL^4	345.6	31.1 (30.2)	313.4	80.3	357.4	−74.3	C_6H_4, 2HCN
NiL^1	421.9	27.6 (28.4)	439.3	94.3	–	–	C_6H_4, HCN
NiL^2	420.2	16.1 (16.2)	–	–	438.6	−361.6	C_6H_4
NiL^3	410.0	33.8 (34.1)	256.2	44.2	–	–	C_6H_4, 2HCN, C_2H_5
NiL^4	430.6	51.4 (52.5)	348.8	86.4	–	–	C_6H_4, 2HCN, C_2H_5O

T^a: Onset decomposition temperature from TGA.
[a]Data obtained from TGA; 15°C min^{-1} under N_2 gas.
[b]Data obtained from DSC; 20°C min^{-1} under N_2 gas.

3.5. *Thermal analysis*

The thermal properties of the Schiff bases and their complexes were investigated by TGA and by DSC under nitrogen at the rate of 15 and 20°C min^{-1}, respectively. Transition temperatures, enthalpy changes, and decomposition temperatures of Schiff bases and related metal(II) complexes are tabulated in table 4. The TGA data indicate that H_2L^1, H_2L^2, H_2L^3, and H_2L^4 start decomposition at 244°C, 239°C, 266°C, and 246°C, respectively, indicating H_2L^3 has the greatest stability. The TGA curve of the Cu(II) and Ni(II) complexes exhibited no mass loss up to 318°C, indicating the absence of coordinated solvent and high thermal stability of the complexes. A single decomposition step which involved partial loss of the same set of organic moieties was observed for the metal(II) complexes.

Thermal decomposition of the copper complex (CuL^1) proceeded with a single degradation step. The onset degradation temperature begins at 376.9°C with an estimated mass loss of 23.8% (Calcd = 22.3%), accompanied by an exothermic peak with $t_{max} = 386.5$°C on the DSC curve which reasonably accounted for the combined loss of C_6H_4 and HCN groups. The thermogram of the CuL^2 complex showed a mass loss of 22.4% (Calcd = 21.8%) at the onset degradation temperature of 380.4°C and an exothermic DSC peak in this region, $t_{max} = 380.2$°C, which also corresponds the loss of C_6H_4 and HCN groups. The thermogram of the CuL^3 complex shows an estimated mass loss of 41.5% (Calcd = 42.6%) with a corresponding exothermic peak with $t_{max} = 349.4$°C on the DSC curve which could be attributed to the loss of C_6H_4, 2HCN, C_2H_2, and C_2H_5O groups. The TGA curve of the CuL^4 complex showed single-step decomposition. The onset decomposition temperature begins at 346.6°C with an estimated mass loss of 32.9% (Calcd = 30.2%), attributed to the loss of C_6H_4 and 2HCN groups from the coordinated part of the ligand. An exothermic peak with $t_{max} = 357.4$°C on the DSC curve was observed for this step. The order of thermal stability of the copper complexes, $CuL^2 > CuL^1 > CuL^4 > CuL^3$, corresponds to the reverse order for that of the free ligands, thus coordination seemed to have stabilized the ligands.

In the TGA curve of the NiL[1] complex an estimated mass loss of 27.6% (Calcd = 28.4%) was observed at 421.9°C, attributed to the loss of C_6H_4 and HCN from the organic moiety. The decomposition curve of NiL[2] showed single-step degradation with an onset temperature of 420.2°C and an estimated mass loss of 16.1% (Calcd = 16.2%). The weight loss is attributed to loss of C_6H_4. For this step, an exothermic peak with $t_{\max} = 438.6°C$ in the DSC was observed. The NiL[3] complex was stable up to 410.0°C where the decomposition began. The thermogram of the NiL[3] complex showed a mass loss of 33.8% (Calcd = 34.1%), which corresponds to the loss of C_6H_4, 2HCN, and C_2H_5. The onset of decomposition of the NiL[4] complex occurs at 430.6°C with an estimated mass loss of 51.4% (Calcd = 52.5%), which may be attributed to the loss of C_6H_4, 2HCN, and C_2H_4O. The order of stability of the nickel complexes did not bear any regular sequence to that of the ligands unlike the observation made above for the copper(II) complexes.

DSC studies presented a melting process (endothermic peaks) at 381.5°C, 265.3°C, 313.4°C, 439.3°C, 256.2°C, and 348.8°C for CuL[1], CuL[3], CuL[4], NiL[1], NiL[3], and NiL[4], respectively, which confirmed that these complexes did not melt below 250°C. The complexes with the nitro substituent (CuL[2] and NiL[2]) decomposed (exothermic peaks) without melting. All complexes investigated gave endothermic peaks with ΔH values ranging from as low as 15.4 J g^{-1} for CuL[1] to as high as 94.3 J g^{-1} for NiL[1] (table 3) except for CuL[2] and NiL[2]. The typical thermograms for NiL[4] (TGA and DSC) are presented in figure 2.

3.6. *Biological properties*

The *in vitro* biological screenings of the compounds were done against 10 bacterial strains by the disc diffusion method. Zones of inhibition against the growth of various microorganisms are listed in table 5 and figure 3. Commonly used antibacterial drug chloramphenicol was tested as a positive control and the effect of the uncoordinated metal(II) acetate is also reported. It was found that the inhibitory effects of the Schiff bases and their complexes differed with the species of bacteria. H_2L^1 and H_2L^2 were active against all the bacterial strains tested, with inhibitory zones of 8–14 and 9–14 mm, respectively. Four of the bacterial strains, *P. aeruginosa*, *A. calcoaceuticus anitratus*, *B. subtilis*, and *M. kristinae*, showed resistance to H_2L^4. H_2L^3 was active against all the organisms tested with inhibitory zones of 8–10 mm except *S. aureus* which was resistant to this ligand.

The results of bactericidal screening (table 5) show that the metal(II) complexes exhibited higher zones on inhibition than their corresponding Schiff bases against all the bacterial strains tested except *P. aeruginosa* and *S. aureus*, which show resistance against [CuL[4]]. However, [NiL[1]] showed the highest zone of inhibition of 22 mm against *S. epidermidis* and *M. kristinae*, comparable to the activity of the reference antibiotic while nickel acetate showed greater zone of inhibition (18 mm) against *E. coli* than all the complexes presumably because of its higher molar concentration. The increased activity of the metal(II) complexes can be explained on the basis of Overtones concept [21] and Tweedy's chelation theory [22].

A general observation is that the nickel(II) complexes were more active than the copper(II) complexes while the standard drug, chloramphenicol, exhibited higher antimicrobial activity than the Schiff bases and their metal complexes, with inhibitory

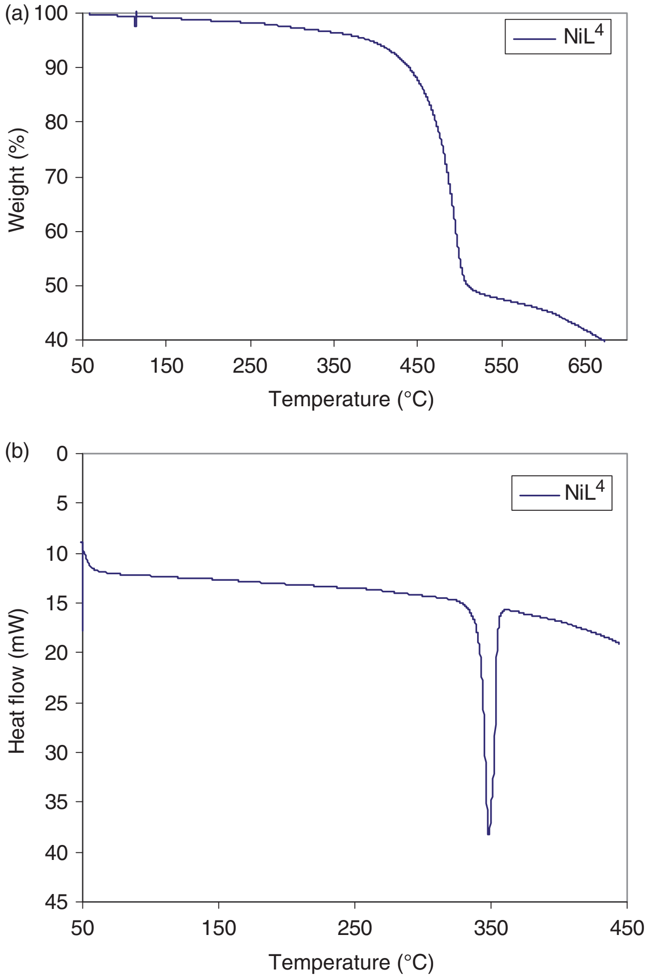

Figure 2. Thermal analysis of NiL^4: (a) TGA and (b) DSC.

zone of 18–30 mm. The enhanced activity of the metal complexes over the ligands complies with trends reported in literature [23, 24].

4. Conclusions

Eight Ni(II) and Cu(II) complexes of unsymmetrical Schiff bases have been synthesized and characterized. The assignment of square-planar geometry to the complexes is corroborated by analytical, spectroscopic, and magnetic susceptibility data. The thermogravimetric studies show that the nickel(II) complexes were more thermally stable than the copper(II) complexes and a single decomposition step, which involves partial loss of the organic moiety, was observed for the metal complexes. A comparative

Table 5. The antibacterial activities of the Schiff bases and their metal complexes.

	Diameter of inhibition zone of bacteria in different compounds (mm)														
Bacterial strains	H_2L^1	NiL^1	CuL^1	H_2L^2	NiL^2	CuL^2	H_2L^3	NiL^3	CuL^3	H_2L^4	NiL^4	CuL^4	$Ni(Ac)_2$	$Cu(Ac)_2$	Chloram phenicol
E. coli	9	12	12	10	8	10	9	8	10	10	10	12	18	10	28
P. aeruginosa	10	10	8	10	10	10	10	10	8	R	10	R	10	8	22
A. calcoaceuticus anitratus	12	14	12	12	12	10	8	12	10	R	12	10	8	12	28
S. flexneri	10	12	10	12	10	10	9	12	12	9	10	12	12	10	22
Salmonella sp.	10	10	14	11	8	10	10	14	12	10	14	12	10	10	22
S. aureus	10	12	10	9	8	8	R	12	12	9	12	R	8	12	26
S. faecalis	9	10	10	9	12	12	10	12	10	10	12	10	12	8	24
B. subtilis	10	12	12	11	12	10	9	10	10	R	10	12	8	R	23
S. epidermidis	10	22	12	10	10	8	9	8	12	11	12	10	12	8	20
M. kristinae	8	22	10	9	8	10	9	8	10	R	10	10	10	R	24

R = Resistant; Ac = Acetate.

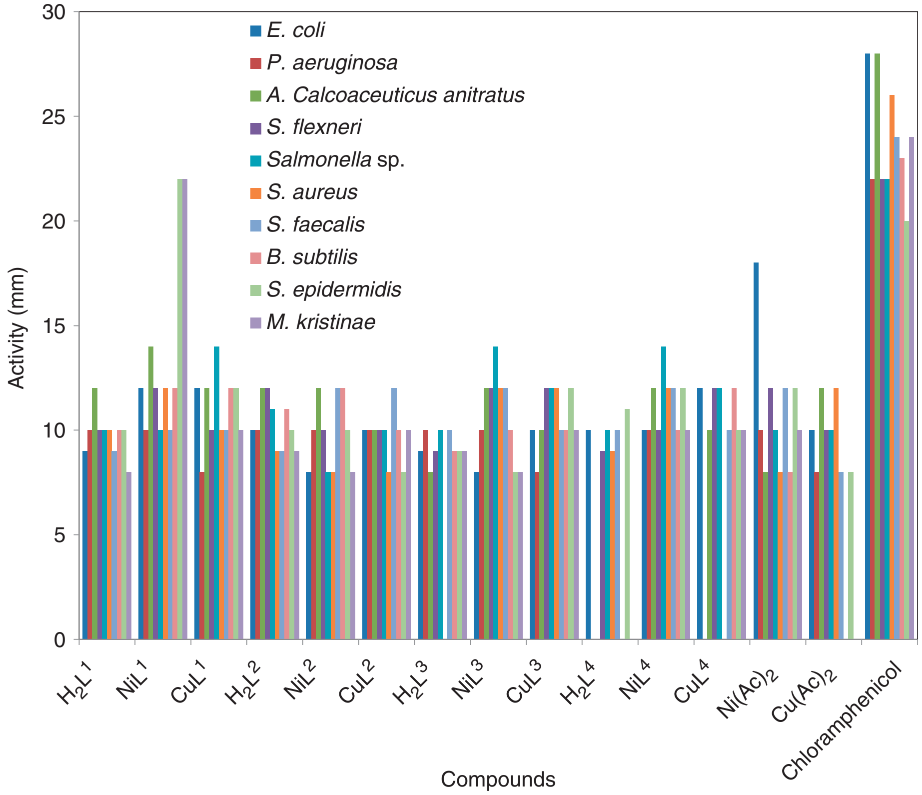

Figure 3. Histogram showing the comparative activities of the compounds.

study of the Schiff bases and their metal(II) complexes showed that the metal(II) complexes exhibited higher antibacterial activity than their corresponding Schiff bases.

Acknowledgments

G.A.K. and A.A.N acknowledge support from the National Research Foundation (NRF), South Africa under the IRDP funding and from University of Zululand Senate research grant.

References

[1] D.H. Brown, W.E. Smith. *Enzyme Chemistry – Impact and Applications*, Chapman and Hall, London (1990).
[2] K. Singh, M.S. Barwa, P. Tyagi. *Eur. J. Med. Chem.*, **42**, 394 (2007).
[3] P.G. Cozzi. *Chem. Soc. Rev.*, **33**, 410 (2004).
[4] S. Chandra, J. Sangeetika. *J. Indian Chem. Soc.*, **81**, 203 (2004).

[5] M.B. Ferrari, S. Capacchi, G. Pelosi, G. Reffo, P. Tarasconi, R. Albertini, S. Pinelli, P. Lunghi. *Inorg. Chim. Acta*, **286**, 134 (1999).
[6] E. Canpolat, M. Kaya. *J. Coord. Chem.*, **57**, 1217 (2004).
[7] M. Yildiz, B. Dulger, S.Y. Koyuncu, B.M. Yapici. *J. Indian Chem. Soc.*, **81**, 7 (2004).
[8] M. Calligaris, G. Nardin, L. Randaccio. *Coord. Chem. Rev.*, **7**, 385 (1972).
[9] J. Costamagna, J. Vargas, R. Latorre, A. Alvarado, G. Mena. *Coord. Chem. Rev.*, **119**, 67 (1992).
[10] S. Yamada, A. Takeuchi. *Coord. Chem. Rev.*, **43**, 187 (1982).
[11] A.D. Garnovskii, A.L. Nivorozhkin, V.I. Minkin. *Coord. Chem. Rev.*, **126**, l (1993).
[12] A.A. Nejo, G.A. Kolawole, A.R. Opoku, C. Muller, J. Wolowska. *J. Coord. Chem.*, **62**, 3411 (2009).
[13] A.W. Bauer, W.N.N. Kirby, J.C. Sherris, M. Turck. *Am. J. Clin. Pathol.*, **45**, 493 (1966).
[14] P.E. Aranha, M.P. Do Santo, S. Romera, E.R. Dockal. *Polyhedron*, **26**, 1373 (2007).
[15] M.M. Abd-Elzar. *J. Chin. Chem. Soc.*, **48**, 153 (2001).
[16] R.D. Hancock, D.A. Thornton. *J. Mol. Struct.*, **4**, 361 (1969).
[17] G.C. Percy, D.A. Thornton. *J. Inorg. Nucl. Chem.*, **34**, 3357 (1972).
[18] G.A. Kolawole, A.A. Osowole. *J. Coord. Chem.*, **62**, 1437 (2009).
[19] D.M. Boghaei, M. Lashanizadegan. *J. Sci. I .R. Iran*, **11:4**, 301 (2000).
[20] X.R. Bu, C.R. Jackson, D.V. Derveer, X.Z. You, Q.J. Meng, R.X. Wang. *Polyhedron*, **16**, 2991 (1997).
[21] N. Dharmaraj, P. Viswanathamurthi, K. Natarajan. *Transition Met. Chem.*, **26**, 105 (2001).
[22] B.G. Tweedy. *Phytopathology*, **55**, 910 (1964).
[23] N. Raman, R. Jeyamurugan, R. Usha Rani, T. Baskaran, L. Mitu. *J. Coord. Chem.*, **63**, 1629 (2010).
[24] A.A. Osowole, G.A. Kolawole, R. Kempe, O.E. Fagade. *Synth. React. Inorg. Met.-Org., Nano-Met. Chem.*, **39**, 165 (2009).